Organic photodetectors with electrically bistable electron acceptors and nanotubes

Satyajit Sahu, Sudip K. Batabyal, and Amlan J. Pal

Articles you may be interested in

Electrical characterization of single-walled carbon nanotubes in organic solar cells by Kelvin probe force microscopy
Appl. Phys. Lett. **96**, 083302 (2010); 10.1063/1.3332489

Effects of semiconducting and metallic single-walled carbon nanotubes on performance of bulk heterojunction organic solar cells
Appl. Phys. Lett. **94**, 233309 (2009); 10.1063/1.3153514

Donor/acceptor type photodetectors: Role of substitution in acceptor material
J. Appl. Phys. **99**, 114503 (2006); 10.1063/1.2199348

Carbon nanotubes-semiconductor networks for organic electronics: The pickup stick transistor
Appl. Phys. Lett. **86**, 182102 (2005); 10.1063/1.1906316

Photocurrent multiplication in organic single crystals
Appl. Phys. Lett. **81**, 1500 (2002); 10.1063/1.1501764

Organic photodetectors with electrically bistable electron acceptors and nanotubes

Satyajit Sahu, Sudip K. Batabyal, and Amlan J. Pal[a)]

Department of Solid State Physics, Indian Association for the Cultivation of Science, Kolkata 700 032,
India and Centre for Advanced Materials, Indian Association for the Cultivation of Science,
Kolkata 700 032, India

The authors provide two routes to increase the photocurrent of organic photodetectors that are based on electron-donor and electron-acceptor materials. During device fabrication, they introduce carbon nanotubes, which act as channels for electron transport. The channels in effect provide an approach to address the problem of low carrier mobility in the conjugated organics. The authors also make use of the (electrically) bistable nature of the acceptor material, namely, rose bengal in a favorable way. During device characterization, they switch its conductivity to decrease device resistance and yield higher photocurrent. Both the routes enhance photocurrent in these donor-acceptor-type photodetectors. © *2007 American Institute of Physics*. [DOI: 10.1063/1.2720296]

In recent years, organic semiconductors are being used in different devices, such as field effect transistors, light-emitting diodes, photovoltaic solar cells, photodetectors, memory elements, etc.[1–3] Most of the devices comprise more than one layer to comply with the operation mechanism for a particular device. In a photodetector, a layer of donor material and a layer of acceptor in sequence are sandwiched between two dissimilar metal electrodes. Photogenerated excitons generally dissociate at the interface between the two layers. Under suitable (reverse) bias, the electrons and holes are transported to the opposite electrodes to yield a photocurrent. So far, low carrier mobility and high device resistance restrict the photocurrent.

As an effort to increase the mobility of carriers, nanomaterials as conducting channels can be introduced in donor or acceptor layers.[4–9] The nanomaterials in the donor and/or acceptor layer provide fast routes for the transport of holes and electrons, respectively, to the opposite electrode. To achieve a higher photocurrent, a decrease in device resistance can be another approach. In order to do so, we introduce an electrically bistable organic material as one of the components of the photodetectors. The inherent conductivity of such molecules can be switched to a high state by application of a suitable voltage pulse.[10,11] The increase in conductivity is generally due to conformational change or electroreduction of the molecules.[12] The photodetector with such a bistable material can hence be "switched on" to yield a higher photocurrent. In this letter, we introduce rose bengal as an electron accepting material, which exhibits electrical bistability. The nanotubes, moreover, act as carrier transporting channels.

Regioregular poly(3-hexyl thiophene) (P3HT) and disodium salt of 4,5,6,7-tetrachloro-2,4,5,7-tetraiodo fluorescein (rose bengal), used as electron donor and electron acceptor, respectively, were purchased from Sigma-Aldrich Fine Chemicals. The regioregularity of the P3HT was 98%. Multiwalled carbon nanotube (CNT), also purchased from the same chemical company, had an outer diameter, wall thickness, length, and purity of 20–30 nm, 1–2 nm, 0.5–2.0 μm, and >95%, respectively. They were acid func-

tionalized following a standard method.[13] Devices were fabricated on indium tin oxide (ITO) coated glass substrates. The P3HT solution in chloroform and rose bengal in methanol (both 0.5 mg/ml) were spun in sequence at 1500 rpm for 30 s. Since the polymer is not soluble in methanol, the deposition of Rose Bengal (RB) did not damage the underneath polymer film. Functionalized CNTs were introduced in an RB layer at different concentrations. The total concentration of RB and CNT in the spinning solution was always 0.5 mg/ml. We hence had four bilayer films, namely, P3HT/RB:CNT, where the CNT concentrations in RB were 0%, 5%, 10%, and 17%. The sum of the thicknesses of P3HT and RB:CNT layers was 50–70 nm.

The films were annealed in vacuum at 50 °C for 2 h before aluminum was thermally evaporated at a pressure below 10^{-5} Torr. The overlap of the electrodes defined the active area of the devices (6 mm^2). Devices were kept in a shielded vacuum chamber with a quartz window. The intensity of the xenon lamp was varied between 10–100 mW/cm^2 with neutral density filters. The devices were characterized under dark and illumination conditions. Current-voltage (*I-V*) characteristics were recorded with a Keithley 486 picoammeter and a Yokogawa 7651 voltage source. A bias was applied with respect to aluminum (Al) electrode with a step voltage of 0.05 V and a scan speed of 2.5 mV/s. Electronic absorption spectra of the films, deposited on quartz substrates, were recorded with an Agilent 8453 UV-Visible spectrophotometer. The microstructure of RB:CNT films was digitized with a JEOL JSM 6700F field emission scanning electron microscope (SEM) showing a homogeneous distribution of the CNTs in a RB matrix (Fig. 1).

Electronic absorption spectra of P3HT, RB:CNT, and P3HT/RB:CNT films are shown in Fig. 2. CNT had a concentration of 17% in the latter two cases. The corresponding spectra show the signature of P3HT and rose bengal. The spectrum of P3HT/RB:CNT is an algebraic sum of the other two, showing that no charge-transfer complex formed at the interface. In addition, it shows that the devices will remain active below 600 nm.

Energy levels of P3HT and rose bengal favor exciton dissociation at the interface. They, along with work functions of ITO and Al electrodes, allow carrier transport to the op-
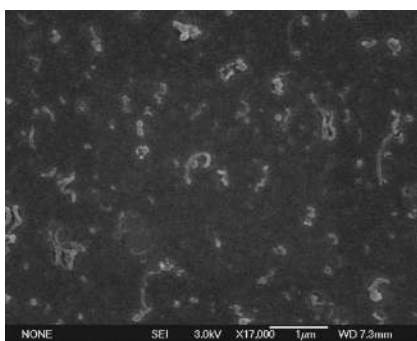

[a)]Electronic mail: sspajp@iacs.res.in

FIG. 1. SEM image of a film containing P3HT/RB:CNT. The concentration of CNT in rose bengal (RB) is 17% by weight.

FIG. 3. (Color online) Current-voltage characteristics of four devices under dark and 100 mW/cm^2 white light illumination. Open symbols represent the dark current of the corresponding devices.

posite direction. The band diagram also affirms that in the reverse bias charge injection from the electrodes is not favorable—that is, they form blocking contacts. Accordingly, ITO/P3HT/RB/Al devices yield very low dark current in the 0–2 V range (Fig. 3). Upon photoexcitation, the devices exhibit a photo current, the magnitude of which increases with bias in a nonlinear fashion. Figure 3 further shows that both photocurrent and dark current increase with the addition of CNT in the RB layer. Here, the CNTs provide channels for electron transport through the RB layer. Since the channels also offer routes for carrier injection from the electrode, the magnitude of the dark current (in the reverse bias) also increases with the increase in CNT concentration. With the introduction of CNT, the quantum of change in the photocurrent is significantly high as compared to the change of the dark current. Since the CNTs do not contribute to the photo-absorption process, a higher photocurrent in the P3HT/RB:CNT device as compared to the P3HT/RB case must mean that the CNTs provide routes for electron transport to the Al electrode. The CNTs, in effect, extract the electrons that are confined in the devices due to their low mobility in rose bengal. The CNTs present near the P3HT layer may also act as exciton dissociating centers. Overall, the results establish the advantages of using CNTs in augmenting the photocurrent of photodetectors.

As another route to increase the photocurrent, we intended to switch the conductivity of rose bengal. The materials in the xanthene class, in which rose bengal is a typical example, exhibit voltage-driven electrical bistability. That is, by applying a suitable voltage pulse, conductance of the material can be switched to a high value. When bias is swept from a negative to a positive voltage, the high-conducting state is retained until a suitable positive bias, at which the molecules' conductivity decreases to the initial (low) value, is reached.
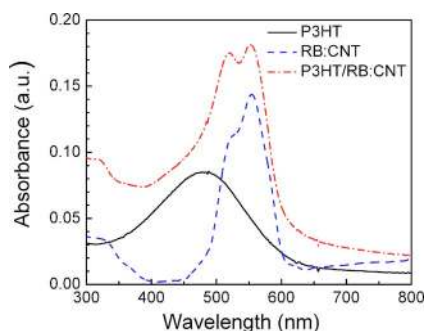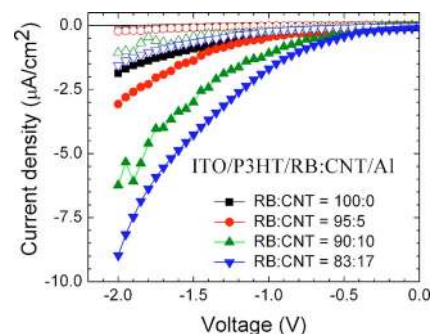
In P3HT/RB:CNT-based photodetectors, we aimed to enhance the conductivity of rose bengal so that the transport of electrons, generated after dissociation of excitons, becomes favorable. Figure 4 shows dark current and photocurrent of such a photodetector (with 17% CNT) before and after conductance switching. A −3.0 V pulse (width, 10 s) was applied to switch the conductivity of rose bengal to a high state. Before and after the −3.0 V pulse, I-V characteristics in dark and illumination conditions were recorded in a suitable voltage range (−3.0 to +2.0 V). The range ensures that once the conductivity of rose bengal molecules is switched to a high level, the molecules do not switch off. The figure shows that due to the decrease in the resistance of the rose bengal layer induced by conductance switching, the magnitude of both dark current and photocurrent in the reverse bias increased. The increase in photocurrent is substantial, showing the advantages of using electrically bistable molecules in photodetectors. When a higher amplitude or width of voltage pulse was used to switch the rose bengal molecules, the characteristics did not change. The initial I-V's could be retrieved only when rose bengal molecules were switched off to its initial low-conducting state by applying a +3 V pulse. This is due to reversible electrical bistability known in rose bengal and similar molecules.

Since electrical bistability is associated with conformational change and electroreduction, the difference between the highest occupied molecular orbitals (HOMOs) and the lowest unoccupied molecular orbitals (LUMOs) of the molecule decreases with switching to a high state.[14] During the process, either the HOMO level would increase, or the LUMO would decrease. Both levels might also change. As a

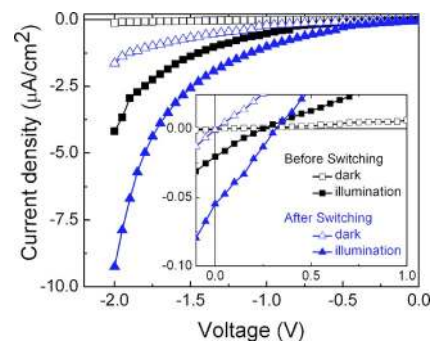FIG. 2. (Color online) Absorption spectra of P3HT, RB:CNT, and P3HT/RB:CNT (17%) films on quartz.

FIG. 4. (Color online) Current-voltage characteristics of a device based on P3HT/RB:CNT (17%) films under dark and 100 mW/cm^2 white light illumination. Measurements were carried out before and after switching of rose bengal. Inset shows a magnified view of the characteristics in the fourth quadrant.
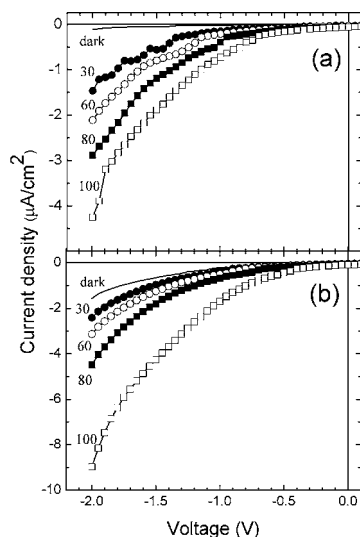
FIG. 5. Current-voltage characteristics of a device based on P3HT/RB:CNT (17%) films under dark and different illumination intensities (as specified in the figures) (a) before and (b) after switching of rose bengal (RB).

FIG. 6. Illumination intensity dependence of current density at −1.0 V before and after conductance switching of rose bengal (RB). The device is based on P3HT/RB:CNT (17%) films. The lines are best fit to the points in the low and high intensity regions.

result, open-circuit voltage (V_{OC}), which is determined by the energy difference between the HOMO of electron donor and the LUMO of electron acceptor, should decrease. In the inset of Fig. 4, we have plotted the fourth quadrant section of all the I-V characteristics to show the V_{OC} and short-circuit current (I_{SC}). The plot illustrates that due to conductance switching, V_{OC} decreases while I_{SC} increases. The increase in I_{SC}, in spite of the decrease in V_{OC}, is due to the large decrease in resistance of the device that occurred during conductance switching of rose bengal molecules.

We have measured the photocurrent of the devices at different illumination intensities. Such measurements were carried out before and after switching the conductance of rose bengal. Since the high-conducting state of the xanthene class materials is stable for hours, we applied a "write" voltage pulse (−3 V, 10 s) only once and have recorded all the I-V characteristics in the dark and at different illumination conditions. Figures 5(a) and 5(b), showing I-V characteristics before and after conductance switching of rose bengal, respectively, demonstrate that the contribution of the switching was evident at all illumination intensities. At any bias or light intensity, the photocurrent increased due to conductance switching. The results show that the new route to enhance photocurrent is applicable to the entire bias and light intensity regions.

The intensity dependence of the photocurrent has been summed up in Fig. 6. The current at a particular voltage for the two cases is plotted as a function of light intensity. The intercepts with the y axis represent the dark current for the two cases. For a device, the increase in photocurrent is at least three times higher than the increase in dark current (due to switching). When photocurrents before and after conductance switching are compared, the photocurrent at a voltage is more than double in the latter case. The figure shows that when the illumination intensity is low, the current increases with a slope of unity. This shows that with an increase in light intensity, more excitons are generated, which are successfully dissociated, and subsequently more carriers are transported to the opposite electrodes. At higher light intensity, the slope of the plots rises to 2. This can be due to the
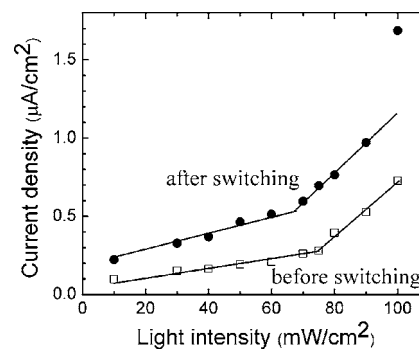
increase in carrier mobility (and consequently higher photocurrent) at higher concentration of charge carriers in the device.

In summary, we have fabricated and characterized photodetectors based on a heterojunction between electron-donor and electron-acceptor layers. To increase the photocurrent, we introduced two routes, namely, (1) incorporated CNTs as channels for electron transport and (2) decreased resistivity of acceptor layer (rose bengal) via conductance switching. With the introduction of CNTs, the photocurrent increases due to the extraction of carriers that are earlier confined in the devices (without CNTs) due to the low mobility of rose bengal. We could further increase the photocurrent by decreasing the overall resistance of rose bengal, which exhibited electrical bistability under a suitable voltage pulse. Light intensity dependences of photocurrent before and after conductance switching show that due to the switching, the photocurrent is enhanced in the entire bias and light intensity regions.

[1] G. Yu, J. Gao, J. C. Hummelen, F. Wudl, and A. J. Heeger, Science **270**, 1789 (1995).
[2] J. J. M. Halls, C. A. Walsh, N. C. Greenham, E. A. Marseglia, R. H. Friend, S. C. Moratti, and A. B. Holmes, Nature (London) **376**, 498 (1995).
[3] P. Peumans, A. Yakimov, and S. R. Forrest, J. Appl. Phys. **93**, 3693 (2003).
[4] S. A. McDonald, G. Konstantatos, S. Zhang, P. W. Cyr, E. J. D. Klem, L. Levina, and E. H. Sargent, Nat. Mater. **4**, 138 (2005).
[5] D. Qi, M. Fischbein, M. Drndić, and S. Šelmić, Appl. Phys. Lett. **86**, 093103 (2005).
[6] W. Feng, Y. Li, Y. Feng, and J. Wu, Nanotechnology **17**, 3274 (2006).
[7] E. Kymakis and G. A. J. Amaratunga, Appl. Phys. Lett. **80**, 112 (2002).
[8] S. Bhattacharyya, E. Kymakis, and G. A. J. Amaratunga, Chem. Mater. **16**, 4819 (2004).
[9] J. U. Lee, Appl. Phys. Lett. **87**, 073101 (2005).
[10] A. Bandhopadhyay and A. J. Pal, J. Phys. Chem. B **107**, 2531 (2003).
[11] F. L. E. Jakobsson, X. Crispin, and M. Berggren, Appl. Phys. Lett. **87**, 063503 (2005).
[12] A. Bandyopadhyay and A. J. Pal, Adv. Mater. (Weinheim, Ger.) **15**, 1949 (2003).
[13] Y. Qin, J. Shi, W. Wu, X. Li, Z. X. Guo, and D. Zhu, J. Phys. Chem. B **107**, 12899 (2003).
[14] A. O. Solak, S. Ranganathan, T. Itoh, and R. L. McCreery, Electrochem. Solid-State Lett. **5**, E43 (2002).